Photochemistry and Photobiology, 2015, 91: 1123–1132

Functional Characterization of a LOV-Histidine Kinase Photoreceptor from *Xanthomonas citri* subsp. *citri* †

Ivana Kraiselburd[1], Alexander Gutt[2], Aba Losi[3], Wolfgang Gärtner[2] and Elena G. Orellano*[1]

[1]Facultad de Ciencias Bioquímicas y Farmacéuticas, Instituto de Biología Molecular y Celular de Rosario (IBR), CONICET, Universidad Nacional de Rosario, Rosario, Argentina
[2]Max-Planck-Institute for Chemical Energy Conversion, Mülheim, Germany
[3]Department of Physics and Earth Sciences, University of Parma, Parma, Italy

Received 26 March 2015, accepted 18 June 2015, DOI: 10.1111/php.12493

ABSTRACT

The blue-light (BL) absorbing protein Xcc-LOV from *Xanthomonas citri* subsp. *citri* is composed of a LOV-domain, a histidine kinase (HK) and a response regulator. Spectroscopic characterization of Xcc-LOV identified intermediates and kinetics of the protein's photocycle. Measurements of steady state and time-resolved fluorescence allowed determination of quantum yields for triplet (Φ_T = 0.68 ± 0.03) and photoproduct formation (Φ_{390} = 0.46 ± 0.05). The lifetime for triplet decay was determined as τ_T = 2.4–2.8 μs. Fluorescence of tryptophan and tyrosine residues was unchanged upon light-to-dark conversion, emphasizing the absence of significant conformational changes. Photochemistry was blocked upon cysteine C76 (C76S) mutation, causing a seven-fold longer lifetime of the triplet state (τ_T = 16–18.5 μs). Optoacoustic spectroscopy yielded the energy content of the triplet state. Interestingly, Xcc-LOV did not undergo the volume contraction reported for other LOV domains within the observation time window, although the back-conversion into the dark state was accompanied by a volume expansion. A radioactivity-based enzyme function assay revealed a larger HK activity in the lit than in the dark state. The C76S mutant showed a still lower enzyme function, indicating the dark state activity being corrupted by a remaining portion of the long-lived lit state.

INTRODUCTION

In living organisms light perception is carried out through photoreceptors that belong to different families based on the structure of their light-absorbing chromophores. LOV (light, oxygen, voltage) domains are BL sensory modules that were originally described in plant phototropins and subsequently found in proteins present in most bacterial species (1,2). The capability to sense BL is given by their flavin chromophore, which in most proteins studied so far, is a flavin mononucleotide (FMN) molecule, although also riboflavin and flavin adenine dinucleotide (FAD) chromophores have been reported (3–5). In the dark-adapted state (referred to as LOV_{450} from the maximum absorption in the visible range), the flavin chromophore is noncovalently bound to the protein moiety. The absorption and fluorescence (emission maximum at *ca* 500 nm) spectra of LOV_{450} are typical for flavin in the oxidized form, with a sharp vibrational pattern due to the rigidity of the binding pocket. Upon UVA or BL absorption, the flavin molecule converts into its triplet state with a quite high quantum yield (Φ_T typically > 0.5) (6). Triplet decay is accompanied by the formation of a covalent bond between position 4a of the flavin ring and a closely located cysteine residue. This photo adduct, referred to as LOV_{390}, shows a strongly blue-shifted absorption spectrum with concomitant loss of the vibrational patterns and fluorescence. LOV_{390} is considered to be the signaling state *in vivo* (6,7). The photo adduct decays thermally to the dark-adapted state with a recovery lifetime (τ_R) varying between seconds and hours depending on the specific protein (5).

Xanthomonas citri subsp. *citri* (Xcc) is a gram-negative bacterium responsible for citrus canker, a severe disease that affects Citrus plants. Xcc genome sequencing revealed a gene encoding a LOV protein composed of an N-terminal LOV domain, associated to a C-terminal histidine kinase domain and a response regulator domain (proteins with such composition are coined hybrid HK - RR) (8). In previous work, we demonstrated that the Xcc-LOV protein is a legitimate BL photoreceptor showing the canonical absorption and fluorescence properties of LOV domains (9). Moreover, Xcc-LOV is involved in the light-dependent regulation of several physiological processes directly involved in the bacterial ability to colonize host plants (9), and counteract plant defense responses (10). Here, we report the molecular properties of Xcc-LOV, employing steady state and time resolved spectroscopic methods for studying the processes leading to photoadduct formation and decay, and we provide information from laser-induced optoacoustic spectroscopy (LIOAS) on thermodynamics and structural changes caused by light absorption. We constructed a protein variant in which the instrumental cysteine residue (C76) was mutated into serine (C76S), allowing for a comparison of the light-driven reactions between both proteins. In addition to determining photophysical and photochemical parameters, we evaluated the functionality of Xcc-LOV as a light-driven protein kinase by radioactivity assays. Comparison of the mutated to the wild-type protein identified a small constitutive activity that is clearly amplified by BL-irradiation.

*Corresponding author email: orellano@ibr-conicet.gov.ar (Elena G. Orellano)
†Part of the data in this paper was presented during the 16th International Congress on Photobiology held in Cordoba, Argentina, in September (8th–12th), 2014.

MATERIALS AND METHODS

Purification of recombinant proteins. The gene encoding the complete Xcc-LOV protein from Xcc was cloned into a pET 28a (+) (Novagene) plasmid rendering the plasmid pet-*lov* (9). The Cysteine 76 to Serine mutation was generated by polymerase chain reaction (PCR) according to the QuikChange method (QuikChange II XL; Stratagene, Cambridge, UK) using the plasmid pet-*lov* as template with primers Lov-cys_1, front: 5′-CATCGGCAACAACAGCCGCTTCCTGC and Lov-cys_2, rear: 5′-GCAGGAAGCGGCTGTTGTTGCCGATG. Polymerase chain reaction products were treated with the restriction enzyme *Dpn*I (New England BioLabs, Herts, UK), and the mutation was confirmed by sequencing. Purification of the wild-type and mutated recombinant proteins was performed as described in Kraiselburd *et al.* (9).

Steady-state spectroscopy. All measurements were performed at 20°C using 1 cm path length quartz cuvettes. Absorption spectra were recorded with a Jasco 7850 UV/Vis spectrophotometer. Some experiments were performed with the aid of light-emiting diodes (LEDs) with emission peaks at 356 nm (LED356), 405 nm (LED405), and 465 nm (LED465) and FWHM of ~25 nm (Roithner Lasertechnik GmbH, Vienna, Austria), as previously described (11). LED465 and LED405 were used for complete dark into light conversion and to establish a photoequilibrium, respectively. LED356 and LED465 were also employed to determine the quantum yield of adduct formation upon UVA and BL excitation. Differential spectra were obtained graphically by subtracting the corresponding absorption spectra (light minus dark). Protein:chromophore ratios for the purified proteins were determined from the Abs_{280} /Abs_{450} ratios, considering the theoretical values for a ratio of 1:1 calculated with ProtParam (Expasy), and taking into account the contribution of the flavin absorbance to the 280 nm peak (12).

Fluorescence measurements were recorded with a Perkin-Elmer LS50 luminescence spectrometer. Excitation spectra were obtained by recording fluorescence emission at 520 nm with excitation wavelengths between 250 and 500 nm. Emission spectra were obtained using excitation wavelengths of 355 and 450 nm, recording fluorescence emission between 450 and 700 nm. Additionally, fluorescence emission was recorded after the specific excitation of tyrosine and tryptophan residues (280 nm) and of only tryptophan residues (295 nm). Fluorescence quantum yields (Φ_F) of the bound flavin were calculated for the Xcc-LOV and C76S proteins using a FMN solution as standard ($\Phi_F = 0.26$) (13).

Quantum yield of adduct formation (Φ_{390}) was determined as previously described, following the time course of fluorescence bleaching at 500 nm upon illumination of the cuvette from the top with LED356 and LED465, by comparison with the values of 0.32 and 0.49 for the YtvA protein of *Bacillus subtilis* for UVA and BL conversion, respectively (14,15). In order to minimize secondary photoconversion during fluorescence measurements, samples were excited at 303 nm.

To evaluate the kinetics of return to the dark state, Xcc-LOV protein was illuminated with BL and then kept in the darkness, recording the fluorescence emission at 500 nm as a function of time (excitation 303 nm). Fluorescence recovery was fitted into a mono-exponential function yielding the lifetime for the dark recovery (τ_R).

Fluorescence anisotropy was analyzed using parallel or perpendicular polarized radiation to excite the protein samples. Excitation was performed at 355 and 450 nm. For each wavelength, fluorescence emission was analyzed in all possible combinations of polarized excitation and detection light beams. Fluorescence anisotropy was calculated according to the following equations:

$$< r > = \frac{(I_{VV} - G \times I_{VH})}{(I_{VV} + 2G \times I_{VH})} \quad (1)$$

$$G = \frac{I_{HV}}{I_{HH}} \quad (2)$$

I_{VV} and I_{VH} correspond to the fluorescence intensity using vertically polarized light for excitation and detecting vertically and horizontally polarized emission, respectively, and I_{HV} and I_{HH} correspond to the fluorescence emission using horizontally polarized light for excitation and detecting vertically and horizontally polarized emission, respectively.

Time-resolved spectroscopy. The instrumental set-up and data handling for laser-flash photolysis is described in Xu *et al.* (16). Measurements were performed with samples of $A_{450} = 0.4–0.5$. For each detected wavelength ten single excitations were averaged to improve S/N ratio. Between individual shots a (partial) recovery time of 1 min was allowed. Control of absorbance at the end of one set of experiments showed no photodamage of the samples.

Time-resolved fluorescence was detected with a single-photon-counting apparatus model FL900 (Edinburgh Analytical Instruments, Livingston, UK). Fluorescence emission was detected at 497 nm with excitation at 450 nm. An aqueous colloidal suspension of silica gel (Ludox) was used as an internal reference standard.

Laser-induced optoacoustic spectroscopy (LIOAS). Protein samples were excited using the frequency-tripled pulse of an Nd/YAG laser (SL 456G, 6 ns pulse duration, 355 nm; Spectron Laser System, Rugby, UK). The cuvette holder FLASH 100 (Quantum Northwest, Spokane, WA) was temperature controlled to ± 0.02°C. The signal was detected by a V103-RM ultrasonic transducer and fed into a 5662 preamplifier (Panametrics, Waltham, MA). The pulse fluence was varied with a neutral density filter and measured with a pyroelectric energy meter (RJP735 head connected to a meter RJ7620 from Laser Precision Corp.). The beam was shaped by a 1 × 12 mm slit, allowing a time resolution of ~60 ns using deconvolution techniques (17). New coccine (Fluka, Neu-Ulm, Germany) was used as calorimetric reference (18). The time evolution of the pressure wave was assumed to be a sum of mono-exponential functions, as previously described (19). The deconvolution of the pressure wave into a sum of exponential functions was performed with Sound Analysis 3000 (Quantum Northwest). The time window was between 20 ns and 5 μs. At a given temperature and for each resolved i-th step the fractional amplitude φ_i is the sum of the fraction of absorbed energy released as heat (α_i) and the structural volume change *per* absorbed Einstein (ΔV_i), according to the following equation (20):

$$\varphi_i = \alpha_i + \frac{\Delta V_i}{E_\lambda} \frac{c_p \rho}{\beta} \quad (3)$$

E_λ is the molar excitation energy, $\beta = (\partial V/\partial T)_p \Delta V$ is the volume expansion coefficient, c_p is the heat capacity at constant pressure, and ρ is the mass density of the solvent. The fractional heat α_i and the structural volume changes ΔV_i have been separated according to the 'two-temperature' method as previously described (14), in this case by measuring at $T_{\beta = 0} = 1.5$°C and $T_{\beta > 0} = 10$ °C.

The LIOAS signals were best fitted to a two-exponential decay function. An unresolved step ($\tau_1 < 20$ ns) is assigned to the formation of the flavin triplet state (subscript T). The short microsecond process corresponds to the triplet decay into the photoadduct (subscript 390).

Energy balance considerations and the results of deconvolution directly provide the products $\Phi_T E_T$ and $\Phi_{DL} E_{390}$ Eqs. (4) and (5), referring to the quantum yield of formation for the triplet state and adduct, respectively, multiplied by the energy level of the two transient species:

$$\Phi_T \frac{E_T}{E_\lambda} = 1 - \alpha_1 - \Phi_F \frac{E_F}{E_\lambda} \quad (4)$$

$$\alpha_2 = \Phi_T \frac{E_T}{E_\lambda} - \Phi_{390} \frac{E_{390}}{E_\lambda} \quad (5)$$

EF is the average energy for the fluorescence emission (232 kJ mol^{-1}) and $E_\lambda = 337$ kJ mol^{-1} is the photonic energy corresponding to $\lambda_{ex} = 355$ nm of excitation wavelength. For detecting LIOAS signals originating from the dark-adapted state of the wild-type protein, 10 shots were averaged, stirring the sample to avoid accumulation of the photoadduct.

Kinase activity. Kinase activity was determined using [γ-^{32}P] ATP. Reactions were performed at 20°C with 20 μg Xcc-LOV or C76S in 100 μL of a reaction buffer containing 50 mM Tris/HCl, pH 7.8, 50 mM KCl, 1 mM dithiothreithol, 0.5 mM $MgCl_2$, 10 μM unlabeled ATP and 0.2 μM [γ-^{32}P] ATP (10 μCi μL^{-1}, Amersham Pharmacia Biotech, Buckinghamshire, UK). At given time points, 10 μL of the reaction mixture were withdrawn and quenched with 10 μL of a stop buffer containing 5 μL of 250 mM Tris/ HCl, pH 6.8, 15 mM EDTA, 30% v/v glycerol, 11% w/v sodium dodecyl sulfate (SDS), 10% v/v 2-mercaptoethanol,

0.02% w/v bromophenol blue. After heating to 55°C for 5 min, radioactive proteins were separated by SDS-polyacrylamide gel electrophoresis. Gels were dried during 2 h at 70°C, placed into an exposure cartridge and covered with an X-ray film. Autoradiograms were obtained after 1 h exposition at room temperature. Quantification of radioactivity incorporation was performed by a digital image analysis of the luminosity density of the bands reveled in the autoradiograms (luminosity/pixel area) using the histogram function of Adobe Photoshop 7.0.

All numeric data were handled and analyzed using Origin Professional version 8.5 (Microcal Software, Northampton, MA).

RESULTS

The Xcc-LOV protein from the plant pathogen *Xanthomonas citri* subsp. *citri* consists of 540 amino acids (molecular mass 59.4 kDa) and includes an N-terminal LOV domain (aa 39–142), a histidine kinase domain (HK, aa 167–396) and a C-terminal response regulator domain (RR, aa 417–533), rendering this protein a member of the hybrid histidine kinases subfamily of bacterial two component signal transduction systems (3,21). The amino acid sequence of Xcc-LOV when aligned with LOV domains from several bacterial LOV proteins and those from plant Phototropins identifies the amino acids instrumental for LOV protein structure and photochemistry (14) (Fig. 1). Besides the characteristic GXNCRFLQ motif containing the conserved cysteine residue involved in the covalent adduct formation (9), Xcc-LOV protein contains all ten super-conserved amino acids identified in photoactive LOV domains (22). In addition, Xcc-LOV carries a threonine residue at position 44, which was identified as being associated with the classification of LOV proteins in two subfamilies according to their spectral properties in the UVA region of the electromagnetic spectrum. The presence of such residue assigns Xcc-LOV to the group of proteins showing the same UVA pattern as *Avena sativa* phot1-LOV2 and *B. subtilis* YtvA protein (14,15,23). Finally, Xcc-LOV conserves several amino acids that were described to be important for the modulation of the kinetics of formation and decay of the photoadduct, such as asparagine residues at positions 51, 108 and 118 of Xcc-LOV (corresponding to 37, 94 and 104 positions in the YtvA protein, see sequence alignment in Fig. 1) and a glutamine present at position 139 (corresponding to position 123 of YtvA) (19).

Photochemistry of purified Xcc-LOV and C76S proteins

Steady state absorption and fluorescence. All spectroscopic measurements on Xcc-LOV were performed three-fold, using three different protein preparations. The absorption spectrum of the dark-adapted Xcc-LOV protein exhibits the typical characteristics of phot and bacterial LOV domains (22), with absorption peaks at 375, 447, and 475 nm with a sharp vibrational structure (Fig. 2A). The spectral characteristics of the UVA region (a single peak at 375 nm) are similar to those corresponding to the LOV domain from the YtvA protein of *B. subtilis* and the LOV2 domain of Phot1 from *A. sativa*, confirming that Xcc-LOV protein belongs to the same subfamily of LOV proteins, as suggested already based on its amino acid sequence (15,23). Based on the molar extinction coefficient of the protein moiety (ε_{280} = 27500 M^{-1} cm^{-1}) and the contribution of FMN to that wavelength (ε_{280} = 26 200 M^{-1} cm^{-1}), a theoretical value of 4.3 is expected for Abs_{280}/Abs_{447} for a 1:1 protein to chromophore ratio. For Xcc-LOV, this value result of 6.06 $\pm$ 0.63, indicating that the purified protein sample presented a high percentage of bound chromophore (*ca* 70%) although there is a fraction of apoprotein also present.

Protein irradiation with BL resulted in the reversible bleaching of the dark (parental) state with the concomitant formation of a photoproduct absorbing maximally at 390 nm, which can be associated to the formation of the C4a-thiol adduct (LOV_{390}) (22) (Fig. 2A). These features could also be appreciated in the differential spectrum (light minus dark) (Fig. 2B).

The C76S mutant protein showed an absorption spectra akin the dark-adapted wild-type protein with no absorbance change upon irradiation indicating the failure of LOV_{390} formation (not shown). The mutated protein presented a Abs_{280}/Abs_{447} ratio of 5.95 $\pm$ 0.8 (three different sample preparations).

Fluorescence excitation and emission experiments of the dark-adapted Xcc-LOV protein (Fig. 3A,B) yielded parameters typical for LOV domains. Excitation at both 355 and 450 nm yielded an emission at 500 nm, with a shoulder at 523 nm. The Φ_F values, calculated using FMN as standard, were 0.138 $\pm$ 0.018 and 0.152 $\pm$ 0.003 for excitation wavelengths of 355 and 450 nm, respectively (Table 1). These values are similar to those reported for other bacterial LOV proteins (5,24).

As generally found in LOV proteins, illumination of Xcc-LOV resulted in loss of fluorescence (9), consistently with LOV_{390} formation, and thus, its reappearance can be used for determining parental state recovery. Fluorescence recovery was evaluated by keeping the irradiated protein in darkness while recording the fluorescence at 500 nm as a function of time (Fig 3C). Excitation was performed at 303 nm to minimize secondary photochemistry resulting in photoadduct formation.

```
              ▲ ▲      ▲                       ▲▲▲ ▲▲          ▲ ▲       ▲ ▲ ▲              ▲▲▲ ▲
Xcc-LOV    MPMTVTDPHLPDNPIVFANRAFLEMTGYAADEVIGNNCRFLQGPE // ATEVLNYRKDGSSFWNALFISPVFDDKGNLVYFFGSQLDV
BsYtvA     VGVVITDPALEDNPIVYVNQGFVQMTGYETEEILGKNCRFLQGKH // TVQIQNYKKDGTMFWNELNIDPM--EIEDKTYFVGIQNDI
PsLOV-HK   MPMIVTDPNRPDNPIIFSNRAFLEMTGYTAEEILGTNCRFLQGPD // SAEIINYRKDGSSFWNALFISPVYNDAGDLIYFFASQLDI
CcLOVK     MAMIVADATQPDIPIIFANDAFLRLTGYARDEVIGRNCRFLQGPD // AVDLLNYRKDGSPFWNALNMSPVRNDAGQLVYFFGSQVDV
LmLOV      VGVIITDPEQKDNPIIFVNTGFENITGYAKEEALGSNCHFLQGDD // NVLLKNYRKDGTSFMNELTIEPIY-DDHEHLYFVGIQKDV
AsLOV1     QTFVVSDASRPGHPIMYASAGFFNMTGYTSKEVVGRNCRFLQGSG // CGRVLNYKKDGTAFWNLLTIAPIKDEEGRVLKFIGMQVEV
AsLOV2     KNFVITDPRLPDNPIIFASDSFLQLTEYSREEILGRNCRFLQGPE // TVQLINYTKSGKKFWNLFHLQPMRDQKGDVQYFIGVQLDG
             . ::*.   . **:: . .* .:* *  .* :* **:****        :** *.*. * * : : *:  :      *.. * :
```

Figure 1. Sequence alignment of Xcc-LOV (Q8PJH6, aa 39–142) with the LOV domains of YtvA from *Bacillus subtilis* (Bs, O34627, aa 25–126), LOV-HK from *Pseudomonas syringa*e pv tomato (Ps, Q881j7, aa 33–136), LOVK from *Caulobacter crescentus* (Cc, Q9ABE3, aa 33–136), LOV protein from *Listeria monocytogenes* (Lm, P58724, aa 19–121) and with LOV1 (aa 136–239) and LOV2 (aa 413–516) domains of Phot 1 from *Avena sativa* (As, O49003). The threonine residue responsible for the spectral properties of LOV proteins in the UVA region is shown in orange, the conserved cysteine residue involved in photoadduct formation is shown in blue and conserved amino acids involved in the kinetics of LOV photocycle are shown in bold (14,19). The 10 amino acids completely conserved in photoactive LOV domains are highlighted in gray (22). Triangles indicate amino acids that interact with the chromophore. The degree of conservation of residues is indicated as follows: Full (*), strong (:), weak (•) or non-conserved (blank). Access numbers correspond to sequences obtained from the UniProt database.

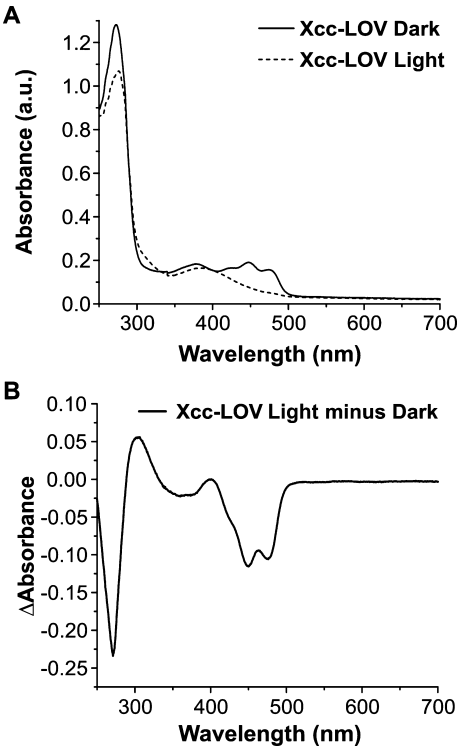

Figure 2. (A) Absorption spectra of the dark-adapted and illuminated (lit) Xcc-LOV protein. (B) Differential spectrum of Xcc-LOV (light minus dark).

The kinetics of recovery of the parental state was fitted to a mono-exponential function yielding a τ_R = 85 min at 20 °C.

Fluorescence emission spectra of the C76S mutant protein (Fig. 4) gave quantum yields Φ_F of 0.27 ± 0.01 and 0.36 ± 0.019 at excitation wavelengths of 355 and 450 nm, respectively (see also Table 1). These values are slightly higher than those obtained for the wild-type protein and more similar to the Φ_F values for free FMN (13). This result is consistent with the absence of the C76 residue, which in the wild-type protein is in close proximity to the chromophore, causing a fluorescence quenching due to its sulfur atom (heavy atom effect).

Additionally, fluorescence emission of tyrosine and tryptophan residues was recorded for the dark-adapted and illuminated Xcc-LOV protein after the excitation at 280 and 295 nm (Fig. 5). In both cases, no differences were observed between the dark and the lit states of Xcc-LOV protein, suggesting that the conformational changes induced upon BL irradiation do not affect the environment of the tyrosine or tryptophan residues.

Fluorescence anisotropy. Fluorescence anisotropy was measured to evaluate the rigidity of the chromophore environment for the Xcc-LOV protein. <*r*> values of 0.285 ± 0.038 and 0.334 ± 0.005 were determined upon excitation at 355 and 450 nm, respectively (three different sample preparations). These values are consistent with those reported for the YtvA protein of *B. subtilis* (14,25). For the C76S mutant protein, <*r*> values resulted of 0.243 and 0.299 for excitation at 355 and 450 nm, respectively (Table 1). These values are slightly lower than those corresponding to the wild-type protein indicating a reduction in the rigidity of the chromophore pocket.

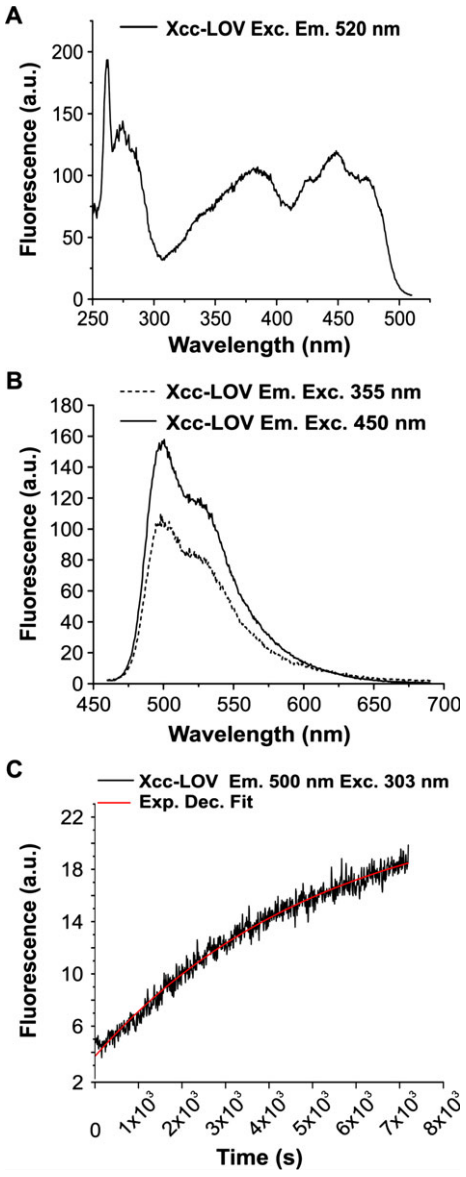

Figure 3. Fluorescence (A) excitation and (B) emission spectra of Xcc-LOV. Emission was recorded between 450–700 nm, with excitation wavelengths of 355 and 450 nm. (C) Dark recovery kinetics of Xcc-LOV (20°C). Experimental data were fitted to a mono-exponential decay function.

Time resolved fluorescence. Fluorescence lifetimes were evaluated by single-photon-counting for the wild-type and the C76S mutant protein and for a FMN solution serving as a standard (Fig. 6). For both proteins fluorescence emission decay was fitted to a bi-exponential function. In the case of Xcc-LOV fluorescence lifetimes resulted as τ_1 = 1.75 ns (for a main component representing the 90.64%) and τ_2 = 7.34 ns (9.36%), whereas for the C76S mutant protein fluorescence lifetimes were τ_1 = 4.15 ns (91.04%) and τ_2 = 8.61 ns (8.86%). Instead, fluorescence of the FMN reference sample decayed mono-exponentially with a 4.4 ns lifetime. We noted that for Xcc-LOV BL illumination does not result in complete loss of fluorescence (data not shown), suggesting that a small quote of the chromophore (*ca* 8–10%) is free or non-specifically bound to the protein, and is not photoconvertible. This could be the reason why we observe such a long lifetime component (τ_2) for <10%

Table 1. Steady-state properties of Xcc-LOV and the C76S mutant protein. Averages arrived from three different sample preparations. λ_{max}: maximum absorption wavelengths; Em_{max}: maximum emission wavelengths; τ_R: lifetime of dark recovery; Φ_F: fluorescence quantum yields; <*r*>: fluorescence anisotropy.

	Xcc-LOV	C76S
λ_{max} (nm)	375, 447, 475	375, 447, 475
λ_{max} (nm) photoadduct	390	–
Em_{max} (nm)	500	500
Φ_F (355 nm Exc.)	0.138 ± 0.018	0.27 ± 0.01
Φ_F (450 nm Exc.)	0.152 ± 0.003	0.36 ± 0.019
τ_R (20°C, min)	85	–
<*r*> (355 Exc.)	0.285 ± 0.038	0.243
<*r*> (450 Exc.)	0.334 ± 0.005	0.299

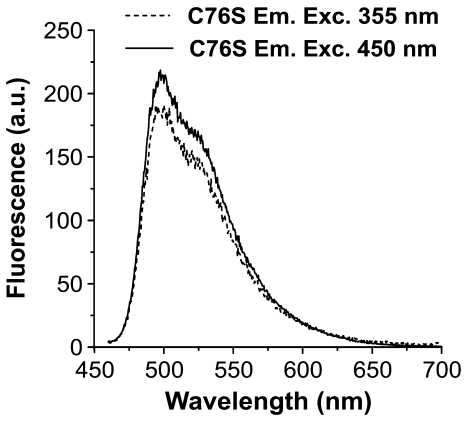

Figure 4. Fluorescence emission spectra of the C76S mutant protein recorded between 450 – 700 nm using excitation wavelengths of 355 and 450 nm.

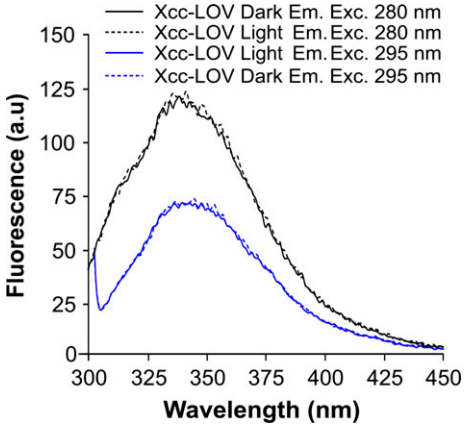

Figure 5. Fluorescence emission of Xcc-LOV protein in either parental (dark) or photoproduct (light) state, recorded between 300–450 nm after the excitation of tyrosine and tryptophan residues (280 nm) and tryptophan alone (295 nm).

of the total fluorescence. The values obtained for Xcc-LOV are very similar to those reported for the YtvA protein of *B. subtilis* (26) (Table 2).

Flash photolysis and LIOAS. Flash photolysis on the Xcc-LOV and the C76S mutant protein identified the decay of the triplet

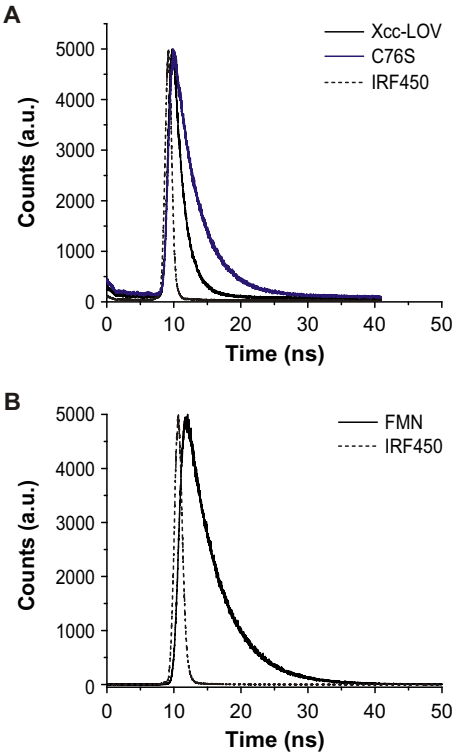

Figure 6. Time resolved fluorescence emission of (A) Xcc-LOV and the C76S mutant protein, and (B) of a reference flavin mononucleotide (FMN) solution. In both cases an aqueous colloidal suspension of silica gel (Ludox) was used for calibration (IRF450). Experimental data were fitted to a bi- (Xcc-LOV and C76S) or mono- (FMN) exponential decay function.

state (its formation being beyond the time-resolution of the detection system), which for the wild-type protein is concomitant with the formation of the photoproduct. The kinetics were detected at several wavelengths (Fig. 7). Mono-exponential fits yielded life times for the wild-type protein of 2.8, 2.9, and 2.4 μs for detection wavelengths of 390, 430, and 620 nm, respectively. The C76S mutant, void of photoproduct formation, showed triplet lifetimes that were longer by nearly a factor of seven: 17. 5, 15.9 and 18.4 μs for 390, 430 and 600 nm, respectively (Table 2).

Laser-induced optoacoustic spectroscopy offers detection of processes shorter than the lower limit of the flash photolysis apparatus employed here, and, in addition, this method provides information on quantum yields, energy content, and volume changes of species occurring during photoconversion. Heat release and structural volume changes detected by LIOAS correspond, for both Xcc-LOV and the C76S mutant protein, to triplet formation that occurs within the shortest (τ_1 < 20 ns) time range accessible by this technique (Fig. 8A,B and Table 2). Quantum yield of triplet formation, Φ_T, could be readily determined in comparison to the triplet state of FMN in solution and within LOV proteins having an energy content E_T = 200 kJ mol^{-1} (15,27). The values obtained were $\Phi_T = 0.68 \pm 0.03$ for Xcc-LOV and $\Phi_T = 0.62 \pm 0.03$ for the C76S mutant protein. Averages arrived from eight deconvolutions and two different sample preparations. As for adduct formation in Xcc-LOV, corresponding to triplet decay, the small amplitude of the associated signal and the quite long lifetime (*ca* 2.8 μs from

Table 2. Properties of LOV proteins and flavin mononucleotide (FMN). Averages arrive from two or three different sample preparations. Data corresponding to wild-type YtvA protein were taken from Losi *et al.* (15) and Gauden *et al.* (27), for its mutant YtvA-C62S from Carmen Mandalari (unpublished data) and for the *Chlamydomonas reinhardtii* phot LOV1 (*Cr*LOV1 wild type and C57S mutant) from Holzer *et al.* (28). τ_1 and τ_2: fluorescence lifetimes; τ_T triplet lifetimes, ΔV_T: volume change associated with triplet formation, Φ_T and Φ_{390}: quantum yields for triplet and photoadduct formation upon BL irradiation, respectively.

	τ_1 (ns) Fluorescence decay	τ_2 (ns) Fluorescence decay	τ_T (μs) Triplet decay	ΔV_T (mL mol^{-1})	Φ_T	Φ_{390}
Xcc-LOV	1.7 (91%)	7.3 (9%)	2.4–2.8	−0.03 ± 0.40	0.68 ± 0.03	0.46 ± 0.05
C76S	4.1 (91%)	8.6 (9%)	16–18.5	−5.1 ± 0.9	0.72 ± 0.03	–
YtvA	2.2 (85%)	4.6 (15%)		−1.5 ± 0.3	0.62 ± 0.10	0.49
YtvA-C62S	2.9 (15%)	4.8 (85%)		−2.9 ± 0.3	0.46 ± 0.03	
*Cr*LOV1	2.9	–		−1.1 ± 0.2	0.63 ± 0.04	
*Cr*LOV1-C57S	4.6	–		−1.7 ± 0.2	0.57 ± 0.05	
FMN	4.4	–		−1.4 ± 0.3	0.6 ± 0.1	

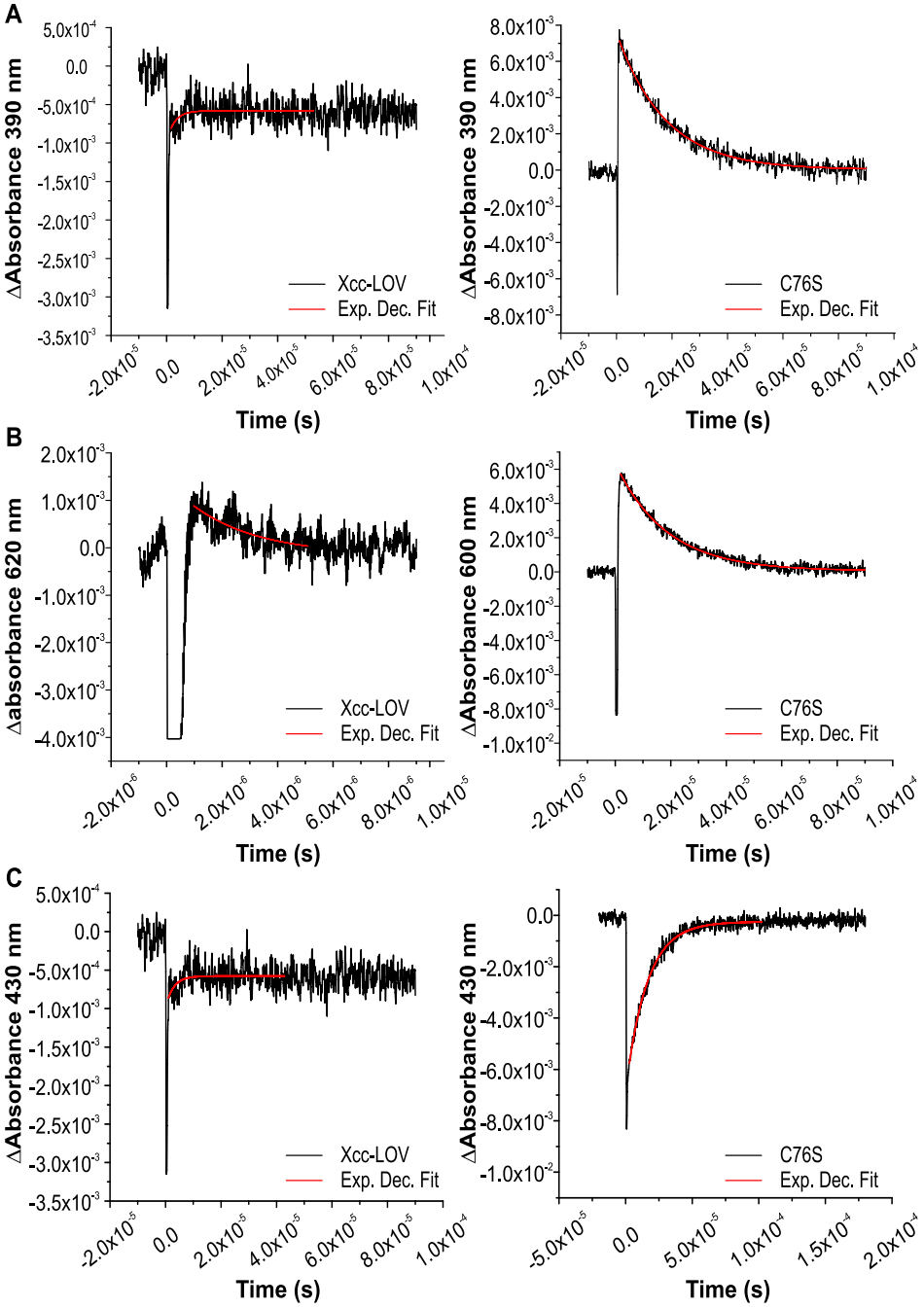

Figure 7. Flash photolysis spectra of the Xcc-LOV (left panels) and the C76S mutant protein (right panels). Transient absorption changes were measured at (A) 390 nm, (B) 620 nm (Xcc-LOV), 600 nm for C76S, and (C) 430 nm. Experimental data were fitted to mono-exponential decay functions.

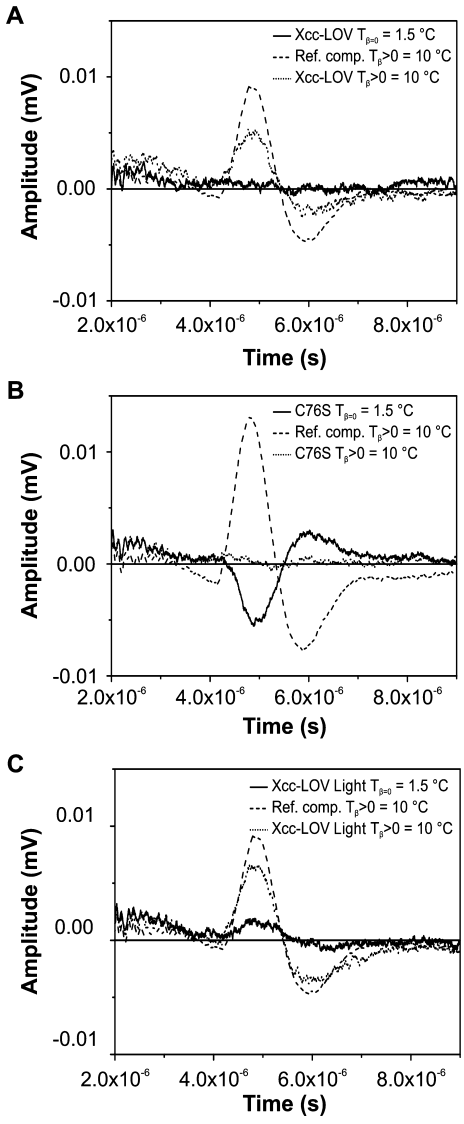

Figure 8. Laser-induced optoacoustic spectroscopy signals for (A) Xcc-LOV, (B) the C76S mutant protein, and (C) the lit state of Xcc-LOV. In (C), the sample was kept illuminated by BL applied from the top of the cuvette. ß: volume expansion coefficient. At $T_\beta = 0 = 1.5$°C the signal for the reference compound is zero (not shown) because the solvent is unable to expand in response to heat deposition ($\beta = 0$). Thus, signals originating from the sample indicate structural volume changes, i.e., being of no thermal origin. Differences in volume changes between the WT protein (minimal contraction), its C76S mutant (pronounced contraction, negative amplitude) and the WT protein in its lit state (expansion, positive amplitude) can clearly be identified.

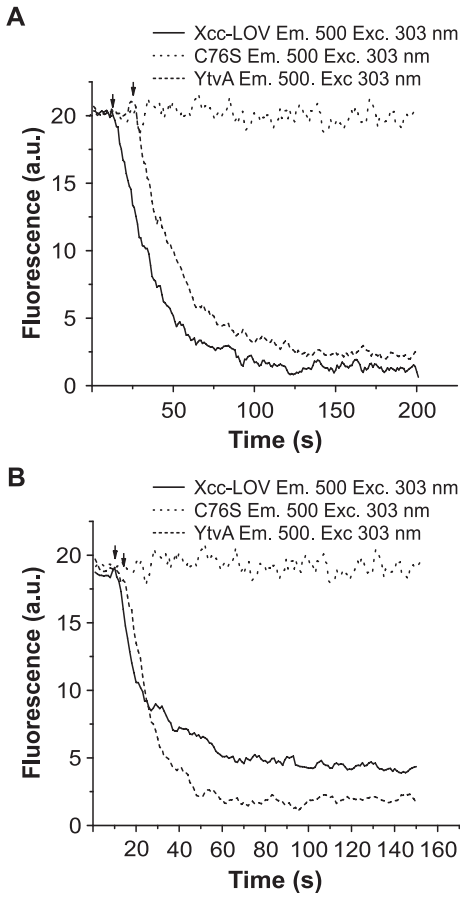

Figure 9. Fluorescence emission of Xcc-LOV, the C76S mutant protein and YtvA recorded at 500 nm as a function of time before and after illumination with (A) blue- or (B) UVA-light for evaluation of the kinetics and quantum yields of photoadduct formation. Arrows represent the moment of sample illumination.

flash-photolysis) hindered straightforward bi-exponential deconvolution, i.e., lifetime and amplitude appeared to be correlated during deconvolution or even undetectable, bearing in mind that the upper time limit of LIOAS is in the order of *ca* 5 μs. As a whole, it appeared not possible to evaluate the thermodynamic parameters of adduct formation for Xcc-LOV by means of LIOAS. It must also be noted that Xcc-LOV behaved differently from LOV proteins previously studied with LIOAS: the structural volume change associated with triplet formation (ΔV_T) did not correspond to a sharp contraction in the wild-type protein (as observed for other LOV proteins), nor was evident a noticeable contraction on a slower time scale associated with photoadduct formation (ΔV_{390}). The values of ΔV_T are normally around -1 to -1.5 mL mol^{-1}, while ΔV_{390} is *ca* -10 mL mol^{-1} (14,15,27). On the other hand, the C76S mutation produced a quite large volume contraction of -5 mL mol^{-1} upon triplet formation, in contrast to free FMN (*ca* -1.4 mL mol^{-1}, see Table 2) and to the corresponding C57S mutation in *Chlamydomonas reinhardtii* phototropin LOV1 (*Cr*LOV1) where $\Delta V_T = -0.9$ mL mol^{-1} (28). Yet, this value is consistent with the corresponding C62S mutation in YtvA, which also produced a larger ΔV_T than in the wild-type protein (Carmen Mandalari, unpublished data, see Table 2).

The apparent absence of a contraction accompanying the triplet state formation is most probably due to a slower conformational process, falling outside of the LIOAS observation time window, as an expansion is clearly detected during the opposite reaction pathway. If a sample in the lit state is laser-excited by ultraviolet light, a photochemical back-reaction can be initiated, being accompanied by an expansion (Fig. 8C and Table 2).

The values of Φ_T were readily calculated by means of LIOAS measurements and Eq. (4), given that the triplet energy level for FMN and LOV proteins is well known (*vide infra*). The determination of quantum yields of adduct formation, Φ_{390}, is more critical because, as mentioned above, for long-lived transients, amplitudes and lifetimes are often correlated or not accessible to

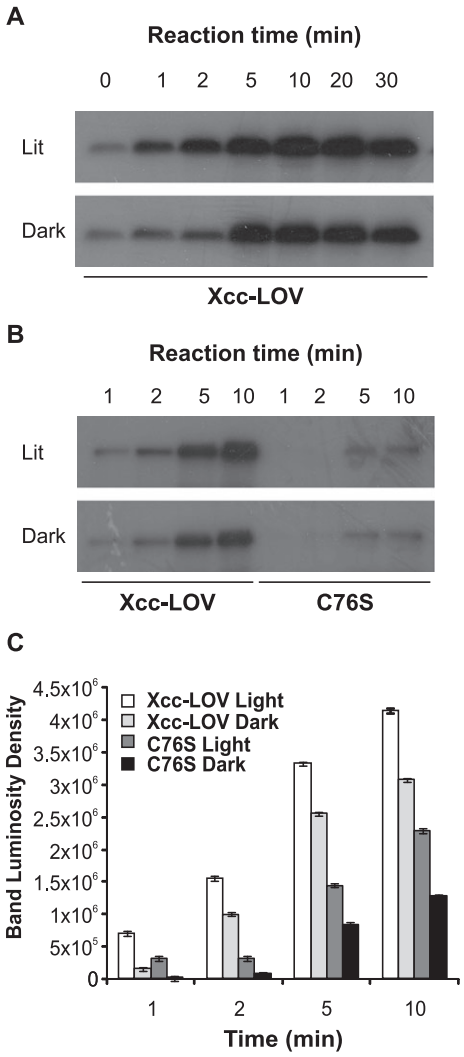

Figure 10. Phosphorylation activity assay for Xcc-LOV (A, B) and the C76S mutant protein (B) under BL irradiation (Light) and in the dark. Autoradiograms show ^{32}P-phosphate incorporation at different reaction times. In (C), the time course of ^{32}P-phosphate incorporation was evaluated after digital image analysis of the luminosity density of the bands reveled in the autoradiograms (luminosity/pixel area). Data correspond to the average of three independent protein samples.

LIOAS. On the other hand, for flash photolysis, the necessity of single shot measurements or low numbers of events for averaging (dictated by the long photocycle) and the small signal amplitude, give rise to a large error in the determination of Φ_{390} (19). Thus, the values of Φ_{390} were determined for Xcc-LOV by following the time course of fluorescence bleaching upon illumination of the cuvette from the top with LEDs emitting at 356 and 465 nm, and by comparison with the well-established values of 0.32 and 0.49 for YtvA (14,15,27) (Fig. 9A,B). In order to minimize photoconversion during fluorescence measurements, samples were excited at 303 nm. The values thus obtained were $\Phi_{390} = 0.33 \pm 0.03$ with LED356 and $\Phi_{390} = 0.46 \pm 0.05$ with LED465 illumination (averaged from three different sample preparations), being fully comparable with values determined for YtvA. In the case of the C76S mutant protein, neither blue nor UVA radiation induced a fluorescence loss, consistently with the involvement of the C76 residue in photoadduct formation (Fig. 9A). UVA illumination results in the establishment of a photoequilibrium, as previously shown for YtvA (11). By comparing volume expansions on the sub-nanoseconds timescale measured with LIOAS for the light-to-dark photoconversion (data not shown), Xcc-LOV appears to be slightly more efficient than YtvA, i.e., with a quantum yield of *ca* 0.1 *vs* 0.05 for YtvA (11).

Kinase activity of Xcc-LOV and C76S proteins. The activity of the HK domain was determined by radioactivity experiments, employing the protein's ability to incorporate radioactive phosphate from [γ-^{32}P] ATP. Each experiment was performed three-fold, using different protein preparations. Phosphate was incorporated by the Xcc-LOV protein both in the light and dark states, but clearly with a higher yield under BL irradiation (Fig. 10A). The phosphorylation reaction reached a plateau within 10 min. For the C76S mutant protein, the yield of phosphate incorporation was found significantly lower than for the wild-type protein in the dark state (Fig. 10B). The mutant protein was able to incorporate a small amount of radioactive phosphate both in the dark and upon light exposure, suggesting an intrinsic basal activity level in the HK domain, which is independent of photoadduct formation. Band intensity density was digitally quantified in order to evaluate the time course of ^{32}Phosphate incorporation (Fig. 10C).

DISCUSSION

The Xcc-LOV protein from the plant pathogen *Xanthomonas citri* subsp. *citri* (540 amino acids) is a three-domain protein composed of a canonical LOV domain, a histidine kinase domain and a fused response regulator, identifying this protein as a member of the hybrid histidine kinases subfamily of bacterial two component signal transduction systems (21). This domain structure is also found in BL photoreceptors from other plant pathogenic bacteria, e.g. *Pseudomonas syringae* pv. syringae or pv. tomato (29). Its LOV domain could be classified to one of two identified LOV-subfamilies according to their spectral properties in the UVA region, belonging to the same family as *A. sativa* phot1-LOV2 and *B. subtilis* YtvA protein (14,15,23). The photochemical properties, determined by steady-state and time resolved absorbance and fluorescence spectroscopy identified the LOV domain as typical for a canonical LOV protein. Interestingly (and still not well understood), the protein moiety does not show noticeable conformational changes upon photo-activation, as demonstrate by the unchanged fluorescence emission for tryptophan and tyrosine residues. This was corroborated by the fluorescence anisotropy. This observation concurs with those for other LOV domains (30,31), leaving us without meaningful explanations for the signal transmission in these proteins. However, a slightly less constringent structure could be determined for the C76S mutant from the fluorescence anisotropy values (excitation at 355 and 450 nm yielding $\langle r \rangle$ values of 0.243 and 0.299, compared to values of 0.285 ± 0.038 and 0.334 ± 0.005 for the wild-type protein). The slightly lower values determined for the mutant protein indicate a reduction in the rigidity of the chromophore pocket upon mutation of the instrumental cysteine. This finding is in agreement with observations for YtvA protein of *B. subtilis* (14,25).

Time-resolved absorbance changes (laser flash photolysis), combined with optoacoustic spectroscopy yielded information on the early processes of the photochemical reaction. The

photoproduct was formed from triplet decay with consistent lifetimes determined at different wavelengths (2.4–2.8 μs). In case the photoproduct formation is blocked upon conversion of the reactive cysteine into serine, the triplet lifetime is significantly longer. Laser-induced optoacoustic spectroscopy measurements also allowed determining an upper limit (≤20 ns) and the quantum yield for triplet formation ($\Phi_T = 0.68 \pm 0.03$), and in combination with fluorescence decay kinetics upon irradiation, also the quantum yield for the photoproduct formation ($\Phi_{390} = 0.46 \pm 0.05$ for 465 nm irradiation and $\Phi_{390} = 0.33 \pm 0.03$ for 356 nm irradiation) could be determined. Again these values, differing for the two excitation wavelengths showed a lower quantum yield upon ultraviolet over blue light excitation. Seen also for other LOV domains the origin of this difference is not well understood. Xcc-LOV behaved differently to other LOV proteins studied so far by LIOAS as neither the structural volume change associated with triplet formation (ΔV_T) could be associated to a sharp contraction, nor was evident a contraction on a slower time scale associated with photoadduct formation (ΔV_{390}) (14,15,27). Curiously, the C76S mutation produced a quite large volume contraction upon triplet formation, opposite to free FMN and to the corresponding mutation in the instrumental cysteine of *C. reinhardtii* phototropin LOV1 (*Cr*LOV1) (28). Notably, also in YtvA the corresponding C62S mutation induces a larger ΔV_T than in the wild-type protein (Carmen Mandalari, unpublished data), which follows the same trend as seen here for Xcc-LOV. The volume contraction associated to adduct formation in the WT protein most probably falls at the very limit of the time-window for LIOAS or its absolute value is very small. However, the reasons for this apparently anomalous behavior of Xcc-LOV cannot be easily inferred by sequence analysis or other absorbance or fluorescence measurements, instead, it would require a thorough investigation with photocalorimetric techniques other than LIOAS that have access to a more extended time window.

The proposal of a retarded contraction for the forward reaction (falling outside of the observation time window) is supported by the finding of an expansion when performing the opposite reaction (light-induced photoproduct to dark state conversion). Interestingly, the LOV domain of Xcc-LOV can be reconverted into the parental state by ultraviolet light, similarly as reported for YtvA (11).

Of major importance for this study is the combination of a detailed photochemical characterization with the determination of the HK enzyme activity. We could clearly demonstrate a light-induced up-regulation of the kinase function, keeping in mind that the slow recovery of the lit state into the parental form could result on a remaining portion of the lit state that might be misinterpreted as a residual activity of the dark state. Such argument is further supported by the comparison of the dark state activity with the C76S mutant for which the remaining kinase activity is practically absent. The kinetics of phosphate incorporation is relatively rapid, already after *ca* 10 min the reaction comes to a stand-still, indicating that all kinase molecules are fully loaded.

This study adds molecular details to the formerly reported effects of BL on the physiology and infectivity of Xcc (9,10). It ascribes the observed light-regulated changes on the lifestyle of this plant pathogen to the activity of its light-regulated HK domain and adds important kinetic and thermodynamic parameters to the formerly described phenomenological BL effects. The light-regulated HK of Xcc-LOV can be considered an example of the important role of light, in particular BL, for the infectivity of a pathogen that infects economically relevant plants.

Acknowledgements—This work has been supported by Agencia Nacional de Promoción Científica y Tecnológica (ANPCyT PICT 2010-1762 to EGO), Consejo Nacional de Investigaciones Científicas y Técnicas (CONICET, Argentina) and the European Molecular Biology Organization (EMBO).

REFERENCES

1. Briggs, W. R. and E. Huala (1999) Blue-light photoreceptors in higher plants. *Annu. Rev. Cell Dev. Biol.* **15**, 33–62.
2. Losi, A., C. Mandalari and G. Gawlak (2014) From plant infectivity to growth patterns: The role of blue-light sensing in the prokariotic world. *Plants* **3**, 70–94.
3. Losi, A. (2004) The bacterial counterparts of plant phototropins. *Photochem. Photobiol. Sci.* **3**, 566–574.
4. Zoltowski, B. D., C. Schwerdtfeger, J. Widom, J. J. Loros, A. M. Bilwes, J. C. Dunlap and B. R. Crane (2007) Conformational switching in the fungal light sensor vivid. *Science* **316**, 1054–1057.
5. Losi, A. and W. Gartner (2011) Old chromophores, new photoactivation paradigms, trendy applications: Flavins in blue light-sensing photoreceptors (dagger). *Photochem. Photobiol.* **87**, 491–510.
6. Swartz, T. E., S. B. Corchnoy, J. M. Christie, J. W. Lewis, I. Szundi, W. R. Briggs and R. A. Bogomolni (2001) The photocycle of a flavin-binding domain of the blue light photoreceptor phototropin. *J. Biol. Chem.* **276**, 36493–36500.
7. Crosson, S. and K. Moffat (2001) Structure of a flavin-binding plant photoreceptor domain: Insights into light-mediated signal transduction. *Proc. Natl Acad. Sci. USA* **98**, 2995–3000.
8. Da Silva, A. C., J. A. Ferro, F. C. Reinach, C. S. Farah, L. R. Furlan, R. B. Quaggio, C. B. Monteiro-Vitorello, M. A. Van Sluys, N. F. Almeida, L. M. Alves, A. M. Do Amaral, M. C. Bertolini, L. E. Camargo, G. Camarotte, F. Cannavan, J. Cardozo, F. Chambergo, L. P. Ciapina, R. M. Cicarelli, L. L. Coutinho, J. R. Cursino-Santos, H. El-Dorry, J. B. Faria, A. J. Ferreira, R. C. Ferreira, M. I. Ferro, E. F. Formighieri, M. C. Franco, C. C. Greggio, A. Gruber, A. M. Katsuyama, L. T. Kishi, R. P. Leite, E. G. Lemos, M. V. Lemos, E. C. Locali, M. A. Machado, A. M. Madeira, N. M. Martinez-Rossi, E. C. Martins, J. Meidanis, C. F. Menck, C. Y. Miyaki, D. H. Moon, L. M. Moreira, M. T. Novo, V. K. Okura, M. C. Oliveira, V. R. Oliveira, H. A. Pereira, A. Rossi, J. A. Sena, C. Silva, R. F. De Souza, L. A. Spinola, M. A. Takita, R. E. Tamura, E. C. Teixeira, R. I. Tezza, S. M. Dos Trindade, D. Truffi, S. M. Tsai, F. F. White, J. C. Setubal and J. P. Kitajima (2002) Comparison of the genomes of two *Xanthomonas* pathogens with differing host specificities. *Nature* **417**, 459–463.
9. Kraiselburd, I., A. I. Alet, M. L. Tondo, S. Petrocelli, L. D. Daurelio, J. Monzon, O. A. Ruiz, A. Losi and E. G. Orellano (2012) A LOV protein modulates the physiological attributes of *Xanthomonas axonopodis* pv. *citri* relevant for host plant colonization. *PLoS One*, **7**, e38226.
10. Kraiselburd, I., L. D. Daurelio, M. L. Tondo, P. Merelo, A. A. Cortadi, M. Talon, F. R. Tadeo and E. G. Orellano (2013) The LOV protein of *Xanthomonas citri* subsp. *citri* plays a significant role in the counteraction of plant immune responses during citrus canker. *PLoS One* **8**, e80930.
11. Losi, A., W. Gartner, S. Raffelberg, Z. F. Cella, P. Bianchini, A. Diaspro, C. Mandalari, S. Abbruzzetti and C. Viappiani (2013) A photochromic bacterial photoreceptor with potential for super-resolution microscopy. *Photochem. Photobiol. Sci.* **12**, 231–235.
12. Losi, A., E. Ghiraldelli, S. Jansen and W. Gartner (2005) Mutational effects on protein structural changes and interdomain interactions in the blue-light sensing LOV protein YtvA. *Photochem. Photobiol.* **81**, 1145–1152.
13. Van Den Berg, P. A., J. Widengren, M. A. Hink, R. Rigler and A. J. Visser (2001) Fluorescence correlation spectroscopy of flavins and flavoenzymes: Photochemical and photophysical aspects. *Spectrochim. Acta A Mol. Biomol. Spectrosc.* **57**, 2135–2144.
14. Raffelberg, S., A. Gutt, W. Gartner, C. Mandalari, S. Abbruzzetti, C. Viappiani and A. Losi (2013) The amino acids surrounding the

flavin 7a-methyl group determine the UVA spectral features of a LOV protein. *Biol. Chem.* **394**, 1517–1528.
15. Losi, A., E. Polverini, B. Quest and W. Gartner (2002) First evidence for phototropin-related blue-light receptors in prokaryotes. *Biophys. J* . **82**, 2627–2634.
16. Xu, X., A. Gutt, J. Mechelke, S. Raffelberg, K. Tang, D. Miao, L. Valle, C. Borsarelli, K. Zhao and W. Gartner (2014) Combined mutagenesis and kinetics characterization of the bilin-binding GAF domain of the protein Slr1393 from the Cyanobacterium Synechocystis PCC6803. *ChemBioChem* **15**, 1190–1199.
17. Rudzki, J., J. Goodman and S. Peters (1985) Simultaneous determination of photoreaction dynamics and energetics using pulsed, time resolved photoacoustic calorimetry. *J. Am. Chem. Soc.* **107**, 7849–7854.
18. Abbruzzetti, S., C. Viappiani, D. H. Murgida, R. Erra-Balsells and G. M. Bilmes (1999) Non-toxic, water-soluble photocalorimetric reference compounds for UV and visible excitation. *Chem. Phys. Lett.* **304**, 167–172.
19. Raffelberg, S., M. Mansurova, W. Gartner and A. Losi (2011) Modulation of the photocycle of a LOV domain photoreceptor by the hydrogen-bonding network. *J. Am. Chem. Soc.* **133**, 5346–5356.
20. Rudzki, J., L. J. Libertini and E. W. Small (1992) Analysis of photoacustic waveforms using nonlinear least squares method. *Biophys. Chem.* **42**, 29–48.
21. Qian, W., Z. J. Han and C. He (2008) Two-component signal transduction systems of *Xanthomonas* spp.: A lesson from genomics. *Mol. Plant Microbe Interact.* **21**, 151–161.
22. Mandalari, C., A. Losi and W. Gartner (2013) Distance-tree analysis, distribution and co-presence of bilin- and flavin-binding prokaryotic photoreceptors for visible light. *Photochem. Photobiol. Sci.* **12**, 1144–1157.
23. Salomon, M., J. M. Christie, E. Knieb, U. Lempert and W. R. Briggs (2000) Photochemical and mutational analysis of the FMN-binding domains of the plant blue light receptor, phototropin. *Biochemistry* **39**, 9401–9410.
24. Losi, A. and W. Gartner (2012) The evolution of flavin-binding photoreceptors: An ancient chromophore serving trendy blue-light sensors. *Annu. Rev. Plant Biol.* **63**, 49–72.
25. Losi, A., T. Gensch, M. A. Van Der Horst, K. J. Hellingwerf and S. E. Braslavsky (2005) Hydrogen-bond network probed by time-resolved optoacoustic spectroscopy: Photoactive yellow protein and the effect of E46Q and E46A mutations. *Phys. Chem. Chem. Phys.* **7**, 2229–2236.
26. Mansurova, M., P. Scheercousse, J. Simon, M. Kluth and W. Gartner (2011) Chromophore exchange in the blue light-sensitive photoreceptor YtvA from *Bacillus subtilis*. *ChemBioChem* **12**, 641–646.
27. Gauden, M., S. Crosson, I. H. M. Van Stokkum, R. Van Grondelle, K. Moffat and J. T. M. Kennis (2004) Low-temperature and time-resolved spectroscopic characterization of the LOV2 domain of *Avena sativa* phototropin. In *Femtosecond Laser Applications in Biology*. (Edited By S. Avrilleir and J. M. Tualle), pp. 97–104. Bellingham, WA: SPIE.
28. Holzer, W., A. Penzkofer, M. Fuhrmann and P. Hegemann (2002) Spectroscopic characterization of flavin mononucleotide bound to the LOV1 domain of Phot1 From *Chlamydomonas reinhardtii*. *Photochem. Photobiol.* **75**, 479–487.
29. Cao, Z., V. Buttani, A. Losi and W. Gartner (2008) A blue light inducible two-component signal transduction system in the plant pathogen *Pseudomonas syringae* Pv tomato. *Biophys. J* . **94**, 897–905.
30. Jurk, M., M. Dorn, A. Kikhney, D. Svergun, W. Gartner and P. Schmieder (2010) The switch that does not flip: The blue-light receptor YtvA from *Bacillus subtilis* adopts an elongated dimer conformation independent of the activation state as revealed by A combined AUC And SAXS study. *J. Mol. Biol.* **403**, 78–87.
31. Engelhard, C., S. Raffelberg, Y. Tang, R. P. Diensthuber, A. Moglich, A. Losi, W. Gartner and R. Bittl (2013) A structural model for the full-length blue light-sensing protein YtvA from *Bacillus subtilis*, based on EPR spectroscopy. *Photochem. Photobiol. Sci.* **12**, 1855–1863.